

TASI 2002 lectures on neutrinos

Yuval Grossman

*Department of Physics, Technion–Israel Institute of Technology,
Technion City, 32000 Haifa, Israel*

Abstract

We present a pedagogical review of neutrino physics. In the first lecture we describe the theoretical motivation for neutrino masses, and explain how neutrino flavor oscillation experiments can probe neutrino masses. In the second lecture we review the experimental data, and show that it is best explained if neutrinos are massive. In the third lecture we explain what are the theoretical implications of the data, in particular, what are the challenges they impose on models of physics beyond the SM. We give examples of theoretical models that cope with some of these challenges.

I. INTRODUCTION

The success of the Standard Model (SM) can be seen as a proof that it is an effective low energy description of Nature. We are therefore interested in probing the more fundamental theory. One way to go is to search for new particles that can be produced in yet unreached energies. Another way to look for new physics is to search for indirect effects of heavy unknown particles. In this set of lectures we explain how neutrino physics is used to probe such indirect signals of physics beyond the SM.

In the SM the neutrinos are exactly massless. This prediction, however, is rather specific to the SM. In almost all of the SM extensions the neutrinos are massive and they mix. The search for neutrino flavor oscillation, a phenomenon which is possible only for massive neutrinos, is a search for new physics beyond the SM. The recent experimental indications for neutrino oscillations are indirect evidences for new physics, most likely, at distances much shorter than the weak scale.

In the first lecture the basic mechanisms for generating neutrino masses are described and the ingredients of the SM that ensure massless neutrinos are explained. Then, the neutrino oscillation formalism is developed. In the second lecture the current experimental situation is summarized. In particular, we describe the oscillation signals observed by solar neutrino experiments, atmospheric neutrino experiments and long baseline terrestrial neutrino experiments. Each of these results separately can be accounted for by a rather simple modification to the SM. Trying to accommodate all of them simultaneously, however, is not trivial. In the third lecture we explain what are the theoretical challenges in trying to combine all the experimental indications for neutrino masses, and give several examples of models that cope with some of these challenges.

These lecture notes are aimed to provide an introduction to the topic of neutrino physics. They are not meant to be a review. Therefore, many details are not given and many references are omitted. There are many textbooks [1] and reviews [2, 3, 4] about neutrinos. There is also a lot of information about neutrinos on the web [5, 6]. All these sources provide more detailed discussions with complete set of references on the topics covered in these lectures. Moreover, they also cover many subjects that are not mentioned here.

In preparing the lectures I used mainly the recent review by Gonzalez-Garcia and Nir [4]. This review is a very good starting point to anyone who wants to learn more about neutrino physics.

II. NEUTRINO MASSES

A. Fermion masses

In general, there are two possible mass terms for fermions: Dirac and Majorana mass terms. All fermions can have Dirac mass terms, but only neutral fermions can have Majorana mass terms. Indeed, all the massive fermions in the SM, the quarks and charged leptons, have Dirac mass terms. The neutrinos, however, while massless in the SM, can have both Dirac and Majorana mass terms.

Dirac masses couple left and right handed fields

$$m_D \overline{\psi}_L \psi_R + h.c., \quad (2.1)$$

where m_D is the Dirac mass and ψ_L and ψ_R are left and right handed Weyl spinor fields, respectively. Note the following points regarding eq. (2.1):

- Consider a theory with one or more exact $U(1)$ symmetries. The charges of $\overline{\psi}_L$ and ψ_R under these symmetries must be opposite. In particular, the two fields can carry electric charge as long as $Q(\psi_L) = Q(\psi_R)$.
- Since ψ_L and ψ_R are different fields, there are four degrees of freedom with the same mass, m_D .
- When there are several fields with the same quantum numbers, we define the Dirac mass matrix, $(m_D)_{ij}$

$$(m_D)_{ij} \overline{(\psi_L)}_i (\psi_R)_j + h.c., \quad (2.2)$$

where $i(j)$ runs from one to the number of left (right) handed fields with the same quantum numbers. In the SM, the fermion fields are present in three copies, and the Dirac mass matrices are 3×3 matrices. In general, however, m_D does not have to be a square matrix.

A Majorana mass couples a left handed or a right handed field to itself. Consider ψ_R , a SM singlet right handed field. Its Majorana mass term is

$$m_M \overline{\psi}_R^c \psi_R, \quad \psi^c = C \overline{\psi}^T, \quad (2.3)$$

where m_M is the Majorana mass and C is the charge conjugation matrix [7]. A similar expression holds for left handed fields. Note the following points regarding eq. (2.3):

- Since only one Weyl fermion field is needed in order to generate a Majorana mass term, there are only two degrees of freedom that have the same mass, m_M .

- When there are several neutral fields, m_M is promoted to be a Majorana mass matrix

$$(m_M)_{ij}(\overline{\psi_R^c})_i(\psi_R)_j. \quad (2.4)$$

Here, i and j runs from one to the number of neutral fields. A Majorana mass matrix is symmetric.

- The additive quantum numbers of $\overline{\psi_R^c}$ and ψ_R are the same. Thus, a fermion field can have a Majorana mass only if it is neutral under all unbroken local and global $U(1)$ symmetries. In particular, fields that carry electric charges cannot acquire Majorana masses.
- We usually work with theories where only local symmetries are imposed. In such theories global symmetries can only be accidental. A Majorana mass term for a fermion field ψ breaks all the global $U(1)$ symmetries under which the fermion is charged.

B. Neutrino masses in the SM

The SM is a renormalizable four dimensional quantum field theory where

- The gauge group is $SU(3)_C \times SU(2)_L \times U(1)_Y$.
- There are three generations of fermions

$$\begin{aligned} Q_L(3, 2)_{+1/6}, & \quad U_R(3, 1)_{+2/3}, & \quad D_R(3, 1)_{-1/3}, \\ L_L(1, 2)_{-1/2}, & \quad E_R(1, 1)_{-1}. \end{aligned} \quad (2.5)$$

We use the $(q_C, q_L)_{q_Y}$ notation, such that q_C is the representation under $SU(3)_C$, q_L is the representation under $SU(2)_L$ and q_Y is the $U(1)_Y$ charge.

- The vev of the scalar Higgs field, $H(1, 2)_{+1/2}$, leads to the Spontaneous Symmetry Breaking (SSB)

$$SU(2)_L \times U(1)_Y \rightarrow U(1)_{EM}. \quad (2.6)$$

The SM has four accidental global symmetries: baryon number (B) and lepton flavor numbers (L_e , L_μ and L_τ). It is also convenient to define total lepton number as $L = L_e + L_\mu + L_\tau$, which is also conserved in the SM. An accidental symmetry is a symmetry that is not imposed on the action. It is there only due to the field content of the theory and by the requirement of renormalizability. If we would not require the theory to be renormalizable, accidental symmetries would not be present. For example, in the SM dimension five and six operators break lepton and baryon numbers.

The SM implies that the neutrinos are exactly massless. There are several ingredients that combine to ensure it:

- The SM does not include fields that are singlets under the gauge group, $N_R(1, 1)_0$. This implies that there are no Dirac mass terms $\langle \tilde{H} \rangle \overline{\nu}_L \nu_R$.¹ (We define $\tilde{H} \equiv i\tau_2 H^*$.)
- There are no scalar triplets, $\Delta(1, 3)_1$, in the SM. Therefore, Majorana mass terms of the form $\langle \Delta \rangle \overline{\nu}_L^c \nu_L$ cannot be written.
- The SM is renormalizable. This implies that no dimension five Majorana mass terms of the form $\langle H \rangle \langle H \rangle \overline{\nu}_L^c \nu_L$ are possible.
- $U(1)_{B-L}$ is an accidental non-anomalous global symmetry of the SM. Thus, quantum corrections cannot generate Majorana $\langle H \rangle \langle H \rangle \overline{\nu}_L^c \nu_L$ mass terms.²

Both the neutrinos and the $SU(3)_C \times U(1)_{EM}$ gauge bosons are massless in the SM. There is, however, a fundamental difference between these two cases. The symmetry that protects the neutrinos from acquiring masses is lepton number, which is an accidental symmetry. Namely, one does not impose it on the SM. In contrast, the photon and gluon are massless due to local gauge invariance, which is a symmetry that one imposes on the theory. This difference is significant. An imposed symmetry is exact also when one considers possible new physics at very short distances. Accidental symmetries, however, are likely to be broken by new heavy fields.

One can understand the result that the neutrinos are massless in the SM in simple terms as follows. For a massive particle one can always find a reference frame where the particle is left handed and another reference frame where it is right handed. Thus, in order to have massive neutrinos, the SM left handed neutrino fields should couple to right handed fields. There are two options for such couplings. First, the SM left handed neutrinos can couple to right handed SM singlet fermions. This is not allowed in the SM just because there are no such fields in the SM. The second option is to have couplings between the left handed neutrinos and the right handed anti-neutrinos. Such couplings break lepton number. The fact that lepton number is an accidental symmetry of the SM forbids also this possibility.

¹ Our notation is such that we use capital letters to denote fields before SSB and lowercase Greek or Roman letters to denote the fields after SSB. While such differentiation is meaningful only to field that are charged under the SM gauge group, we use this convention also for SM singlets.

² Note that $U(1)_{B-L}$ has gravitational anomalies. Namely, once gravity effects are included the symmetry is broken and neutrino masses can be generated. The SM, however, does not include gravity. What we learn is that it is likely that the neutrinos are massive in any SM extension that include gravity, in particular, in the real world.

C. Neutrino masses beyond the SM

Once the SM is embedded into a more fundamental theory, some of its properties mentioned above are lost. Therefore, in many SM extensions the neutrinos are massive. Neutrino masses can be generated by adding light or heavy fields to the SM. (By light we refer to fields that have weak scale or smaller masses, while heavy means much above the weak scale.) When light fields are added the resulting neutrino masses are generally too large and some mechanism is needed in order to suppress them. New heavy fields, on the contrary, generate very small masses to the neutrinos. We are now going to elaborate on these two possibilities.

There are two kinds of light fields that can be used to generate neutrino masses. First, right handed neutrino fields, $N_R(1, 1)_0$, couple to the SM left handed lepton fields via the Yukawa couplings and generate Dirac masses for the neutrinos

$$y_N \tilde{H} \overline{L}_L N_R + h.c. \quad \Rightarrow \quad m_D \overline{\nu}_L \nu_R, \quad (2.7)$$

where y_N is a dimensionless Yukawa coupling and the symbol “ \Rightarrow ” indicates electroweak SSB. This mechanism offers no explanation why the neutrinos are so light and why the right handed neutrinos do not acquire large Majorana masses. Another way to generate neutrino masses is to add to the SM a scalar triplet, $\Delta(1, 3)_1$. Assuming that the neutral component of this triplet acquires a vev, a Majorana mass term is generated

$$\lambda_N \Delta \overline{L}_L^c L_L \quad \Rightarrow \quad m_N \overline{\nu}_L^c \nu_L, \quad (2.8)$$

where λ_N is a dimensionless coupling. In that case it remains to be explained why the triplet vev is much smaller than the SM Higgs doublet vev. Note that the triplet vev is required to be small not only to ensure light neutrinos but also from electroweak precision data, in particular, from the measurement of the ρ parameter [8].

The other way to generate neutrino masses is to add new heavy fields to the SM. In that case the low energy theory is the SM, but the full high energy theory includes new fields. Using an effective field theory approach, the effects of these heavy fields are described by adding non-renormalizable terms to the SM action. All such terms are suppressed by powers of the small parameter v/M . Here v is the SM Higgs vev, which characterizes the weak scale, and M is the unknown scale of the new physics, which can be, for example, the Planck scale or the GUT scale. Neutrino masses are generated by the following dimension five operator

$$\frac{\lambda}{M} H H \overline{L}_L^c L_L \quad \Rightarrow \quad m_\nu = \lambda \frac{v^2}{M}, \quad (2.9)$$

where λ is a dimensionless coupling.

Note the following points regarding eq. (2.9):

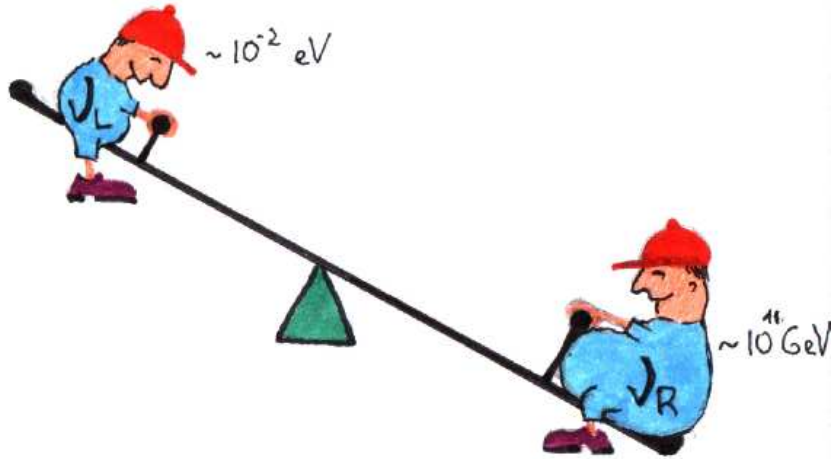


FIG. 1: The seesaw mechanism acquire its name from analogy with a children seesaw. The lower one child takes its arm of the seesaw, the higher the other child goes. For neutrinos, the larger M_N is, the lighter the neutrino becomes. (I Thank Oleg Khasanov for the figure.)

- Taking the SM to be an effective field theory implies $m_\nu \neq 0$. Since we know that new physics must exist at, or below, the Planck scale, it is rather likely that the neutrinos are massive.
- m_ν is small since it arises from non-renormalizable terms.
- Neutrino masses probe the high energy physics.
- The neutrino acquires Majorana mass. Thus, total lepton number is broken by two units.
- The situation can be generalized to the case of several generations. Then, generically, both total lepton number and family lepton numbers are broken and lepton mixing and CP violation are expected.

A famous example of a realization of this effective field theory description is the seesaw mechanism, see fig. 1. (Historically, it was invented within $SO(10)$ GUT theory, and later implemented in many other models.) Consider one generation SM with an additional fermion singlet $N_R(1, 1)_0$. The following two terms in the Lagrangian are relevant for neutrino masses

$$\frac{1}{2}M_N\overline{N_R^c}N_R + Y_\nu H\overline{L}_L N_R + h.c., \quad (2.10)$$

where $M_N \gg v$ is the Majorana mass of the right handed neutrino. After electroweak symmetry breaking the second term leads to a Dirac mass of the neutrino. In the (ν_L, ν_R^c) basis the neutrino mass matrix is

$$m_\nu = \begin{pmatrix} 0 & m_D \\ m_D & M_N \end{pmatrix}, \quad (2.11)$$

where $m_D \equiv Y_\nu v$. Using

$$\text{Tr}(m_\nu) = M_N, \quad |\det(m_\nu)| = m_D^2, \quad (2.12)$$

to first order in v/M_N we find

$$m_{\nu_R} = M_N \quad m_{\nu_L} = \frac{m_D^2}{M_N}. \quad (2.13)$$

Comparing this result with eq. (2.9) one identifies the new physics scale M with M_N and the new physics coupling λ with Y_ν^2 . We learn that the seesaw mechanism is indeed a realization of the effective field theory approach for neutrino masses.

D. Neutrino mixing

Massive neutrinos generally mix. The neutrino mass terms break the accidental family lepton number symmetries. (Total lepton number is also violated if the neutrinos have Majorana masses.) This phenomenon is very similar to quark mixing in the SM. It is therefore instructive to describe both lepton and quark mixing in parallel.

For quarks, the Cabibbo-Kobayashi-Maskawa (CKM) matrix, V , corresponds to non-diagonal charged current interactions between quark mass eigenstates

$$\frac{g}{\sqrt{2}} (\bar{u}_L)_i V_{ij} \gamma^\mu (d_L)_j W_\mu^+, \quad i = u, c, t, \quad j = d, s, b. \quad (2.14)$$

For leptons, it is common to use two different bases. The flavor basis is defined to be the one where the charged lepton mass matrix and the W interactions are diagonal. In the mass basis both the charged lepton and the neutrino mass matrices are diagonal, but the W interaction is not. In that basis the leptonic mixing matrix U is the analogue of the CKM matrix.³ Namely, it shows up in the charged current interactions

$$\frac{g}{\sqrt{2}} \bar{\ell}_L U_{\ell i} \gamma^\mu (\nu_L)_i W_\mu^-, \quad \ell = e, \mu, \tau, \quad i = 1, 2, 3. \quad (2.15)$$

When working in the mass basis, the formalism of quark and lepton flavor mixings are very similar. The difference between these two phenomena arises due to the way neutrino

³ Recently, in many papers the matrix U is called the Maki-Nakagawa-Sakata (MNS) matrix, U_{MNS} , or the Pontecorvo-Maki-Nakagawa-Sakata (PMNS) matrix, U_{PMNS} , since these authors were the first to discuss leptonic flavor mixing. Others call it the CKM or KM analogue for the lepton sector since Kobayashi and Maskawa were the first to discuss CP violation from such matrices. Here we adopt the notation of [4] and call U the leptonic mixing matrix. The fact that the CKM matrix is denoted by V helps in avoiding confusion.

experiments are done. While quarks and charged leptons are identified as mass eigenstates, neutrinos are identified as flavor eigenstates. Indeed, there are two equivalent ways to think about fermion mixing. For quarks, mixing is best understood as the fact that the W interaction is not diagonal in the mass basis. For leptons, we usually refer to the rotation between the neutrino mass and flavor bases as neutrino mixing.

Note that the indices of the two matrices are of different order. In V the first index corresponds to the up type component of the doublet and the second one to the down type. In U it is the other way around.

In general, U is described by three mixing angles and one Dirac CP violating phase. If the neutrinos are Majorana particles there are in addition two more CP violating phases called Majorana phases. The Majorana phases, however, do not affect neutrino flavor oscillations, and we do not discuss them any further.

SM singlet states can mix with the three SM neutrinos. When the masses of the singlet states are small they can participate in neutrino oscillation. Then, the singlet states are usually called sterile neutrinos while the standard model neutrinos are called active neutrinos.⁴ The mixings between all neutrinos are taken into account by enlarging the mixing matrix U to a $3 \times (n + 3)$ matrix, where n is the number of sterile states.

When the SM singlet states are very heavy (with mass $M \gg v$), they cannot participate in neutrino oscillations. Their couplings to the light neutrino is important since it gives them their masses. Thus, the heavy states are usually referred to as right handed neutrinos. The mixings relevant for neutrino oscillations is described by the matrix U that refers only to the 3×3 sub-matrix that corresponds to the mixing between the mostly active states. The presence of the heavy states affects the theory since in that case the matrix U does not describe the full mixing and, therefore, it is not unitary. This deviation from unitarity, however, is very small, of order v/M , and it is usually neglected.

III. METHODS FOR PROBING NEUTRINO MASSES

The conclusion of the last section is that it is very likely that the neutrinos have very small masses and that they mix. There are several ways to probe neutrino masses and mixing angles. Discussions about astrophysical and cosmological probes of neutrino masses can be found, for example, in [1, 3]. Here we briefly discuss kinematic tests for neutrino masses

⁴ Oscillation occurs only between left handed states, that is, both active and sterile states are left handed. One should not get confused by the fact that the sterile states are left handed; the identification of left handed states as SM doublets and right handed states as SM singlets does not have to be true in theories that extend the SM.

and neutrinoless double beta decay. Then we develop the formalism of neutrino oscillation, which is the most promising way to probe the neutrino masses and mixing angles.

A. Kinematic tests

In decays that produce neutrinos the decay spectra are sensitive to neutrino masses. For example, in $\pi \rightarrow \mu\nu$ the muon momentum is fixed (up to tiny width effects), and it is determined only by the masses of the pion, the muon and the neutrino. To first order in m_ν^2/m_π^2 , the muon momentum in the pion rest frame is given by

$$|\vec{p}| = \frac{1}{2m_\pi} \left(m_\pi^2 - m_\mu^2 - \frac{m_\pi^2 + m_\mu^2}{m_\pi^2 - m_\mu^2} m_\nu^2 \right). \quad (3.1)$$

Since the correction to the massless neutrino limit is proportional to m_ν^2 , the kinematic tests are not very sensitive to small neutrino masses. The current best bounds obtained using kinematic tests are [8]

$$\begin{aligned} m_\nu &< 18.2 \text{ MeV} && \text{from } \tau \rightarrow 5\pi + \nu, \\ m_\nu &< 190 \text{ KeV} && \text{from } \pi \rightarrow \mu\nu, \\ m_\nu &< 2.2 \text{ eV} && \text{from } {}^3\text{H} \rightarrow {}^3\text{He} + e + \bar{\nu}. \end{aligned} \quad (3.2)$$

The sensitivities of neutrino oscillation experiments are much better than these bounds. Note that while oscillation experiments are sensitive to the neutrino mass-squared differences (see below) the kinematic tests are sensitive to the neutrino masses themselves.

B. Neutrinoless double β decay

Neutrino Majorana masses violate lepton number by two units. Therefore, if neutrinos have Majorana masses we expect there are also $\Delta L = 2$ processes. The smallness of the neutrino masses indicates that such processes have very small rates. Therefore, the only practical way to look for $\Delta L = 2$ processes is in places where the lepton number conserving ones are forbidden or highly suppressed. Neutrinoless double β decay where the single beta decay is forbidden is such a process. An example for such processes is

$${}_{76}^{32}\text{Ge} \rightarrow {}_{76}^{34}\text{Se} + 2e^-. \quad (3.3)$$

The only physical background to neutrinoless double β decay is from double β decay with two neutrinos.

Note the following points:

- Since neutrinoless double β decay is a $\Delta L = 2$ process, it is sensitive only to Majorana neutrino masses. Dirac masses conserve lepton number and do not contribute to this decay.
- The neutrinoless double β decay rate is related to the neutrino mass-squared. It is also proportional to some nuclear matrix elements. Those matrix elements introduce theoretical uncertainties in extracting the neutrino mass from the signal, or in deriving a bound if no signal is seen.
- Neutrinoless double β decay is sensitive to any $\Delta L = 2$ operator, not only to the neutrino Majorana masses. Thus, the relation between the Neutrinoless double β decay rate and the neutrino mass is model dependent.
- The best bound derived from neutrinoless double β decay is $m_\nu < 0.34$ eV [9].

C. Neutrino vacuum oscillation

We now turn to the derivation of the neutrino oscillation formalism. We use several assumptions in this derivation. We emphasize, however, that in all practical situations it is correct to use these assumptions and that more sophisticated derivations give the same results (see, for example, [10]).

In an ideal neutrino oscillation experiment, a neutrino beam is generated with known flavor and energy spectrum. The flavor and the energy spectrum is then measured at some distance away. If the flavor composition of the beam changed during the propagation it is a signal of neutrino oscillation, which indicates neutrino masses and mixings.

The flavor of the neutrino is identified via its charged current interaction. It is convenient to express a flavor state in terms of mass states

$$|\nu_\alpha\rangle = \sum_i U_{\alpha i}^* |\nu_i\rangle, \quad (3.4)$$

where Greek indices runs over the flavor states ($\alpha = e, \mu, \tau$) and Roman ones over the mass states ($i = 1, 2, 3$). An initially produced flavor state $|\nu_\alpha\rangle$ evolves in time according to

$$|\nu_\alpha(t)\rangle = \sum_i e^{-iE_i t} U_{\alpha i}^* |\nu_i\rangle, \quad (3.5)$$

where we assume that all the components in the neutrino wave packet have the same momenta ($p_i = p$). For ultra relativistic neutrinos we can use the following approximation

$$E_i \approx p + \frac{m_i^2}{2p}. \quad (3.6)$$

Then, the probability to observe oscillation between flavor α and β is given by

$$P_{\alpha\beta} = |\langle \nu_\beta | \nu_\alpha(t) \rangle|^2 = \delta_{\alpha\beta} - 4 \sum_{i < j} U_{\alpha i} U_{\beta i} U_{\alpha j} U_{\beta j} \sin^2 x_{ij}, \quad (3.7)$$

where in the last step we assumed CP conservation and

$$x_{ij} = \frac{\Delta m_{ij}^2 t}{2p}. \quad (3.8)$$

In many cases the three flavor oscillation is well approximated by considering only two flavors. Then,

$$U = \begin{pmatrix} \cos \theta & \sin \theta \\ -\sin \theta & \cos \theta \end{pmatrix}, \quad (3.9)$$

and for $\alpha \neq \beta$ we obtain

$$P_{\alpha\beta} = \sin^2 2\theta \sin^2 x. \quad (3.10)$$

Since the neutrinos are relativistic we usually use $L = t$, $E = p$ and write

$$x = \frac{2\pi L}{L_{\text{osc}}}, \quad L_{\text{osc}} = \frac{4\pi E}{\Delta m^2}, \quad (3.11)$$

such that L_{osc} is the oscillation length. The following formula is also convenient

$$x \approx 1.27 \left(\frac{\Delta m^2}{\text{eV}^2} \right) \left(\frac{L}{\text{km}} \right) \left(\frac{\text{GeV}}{E} \right). \quad (3.12)$$

The oscillation master formula, eq. (3.10), teaches us the following:

- Longer baseline, L , or smaller energy, E , is needed in order to probe smaller Δm^2 .
- When $L \ll L_{\text{osc}}$ we can approximate $\sin^2 x \sim x^2$. In that case the signal is usually too small to be detected.
- When $L \gg L_{\text{osc}}$ the energy spread of the beam and decoherence effects cause the oscillations to average out. That is, in our formula we should take the average value: $\langle \sin^2 x \rangle = 0.5$. In that case only a lower bound on the mass-squared difference between the two neutrinos can be obtained.

D. Matter effects

When neutrinos travel through matter the oscillation formalism is modified. While neutrinos can scatter off the medium, in almost all relevant cases the scattering cross sections are very small, and the effect of scattering is negligible. The effect we are concentrating on is that of the forward scattering of the neutrinos. Like photons, when neutrinos travel inside a medium they acquire effective masses. There is no energy or momentum exchange

between the neutrinos and the medium. The effect of the medium is that it induces effective masses for the neutrinos.

First we discuss the case of a medium with constant density. Moreover, we consider only matter at low temperature, which implies that it consists of electrons, protons and neutrons. Note that there are no muons, taus and anti-leptons in that case. The charged current interaction between the electron neutrinos and the electrons in the medium induces an effective potential for the neutrinos [11]

$$V_C = \sqrt{2}G_F N_e \approx 7.6 Y_e \left(\frac{\rho}{10^{14} \text{g/cm}^3} \right) \text{eV}, \quad (3.13)$$

where N_e (N_p , N_n) is the number density of electrons (protons, neutrons) and $Y_e = N_e/(N_p + N_n)$ is the relative electron number density. To get a feeling for the size of this potential, note that at the Earth core $\rho \sim 10 \text{g/cm}^3$, which gives rise to $V_C \sim 10^{-13} \text{eV}$.

As we discuss below, the current data indicates that $m_\nu \gtrsim 10^{-3} \text{eV}$, and thus $m_\nu \gg V_C$. This seems to suggest that matter effects are irrelevant. This is, however, not the case since the matter effects arise from vector interactions while masses are scalar operators. The right comparison to make is between m_ν^2 and EV_C where E is the neutrino energy. Since $E \gg m_\nu$ matter effects are enhanced and can be important.

To explain this enhancement, we consider a uniform, unpolarized medium at rest. (Discussion about the general case which includes all types of interactions and arbitrary polarization can be found, for example, in [12].) In that case the neutrino feels the four-vector interaction $V_\mu = (V_C, 0, 0, 0)$. Due to V_C the vacuum dispersion relation of the neutrino, $p_\mu p^\mu = m^2$, is modified as follows

$$(p_\mu - V_\mu)(p^\mu - V^\mu) = m^2 \implies E \approx p + V_C + \frac{m^2}{2p}, \quad (3.14)$$

where the approximation holds for ultra relativistic neutrinos. We learn that the effective mass-squared in matter, m_m^2 , is given by

$$m_m^2 = m^2 + A, \quad A \equiv 2EV_C, \quad (3.15)$$

where we used $p \approx E$. It is the vector nature of the weak interaction that makes the matter effects practically relevant.

Interactions that are flavor universal only shift the neutrino energy by a negligibly small amount and do not affect the oscillation. Non-universal interactions, however, are important since in their presence the values of the effective masses and mixing angles are different from their vacuum ones. While the weak neutral current is flavor universal, the charged current is not. In normal matter, where there are electrons but not muons and taus, only electron neutrinos interact via the charged current with the medium. The mixing matrix is modified

by this non-universal matter effect such that the effective squared mass difference and mixing angle are given by

$$\begin{aligned}\Delta m_m^2 &= \sqrt{(\Delta m^2 \cos 2\theta - A)^2 + (\Delta m^2 \sin 2\theta)^2}, \\ \tan 2\theta_m &= \frac{\Delta m^2 \sin 2\theta}{\Delta m^2 \cos 2\theta - A},\end{aligned}\tag{3.16}$$

where the subindex m stand for matter. The oscillation probability is then obtained from (3.10) by replacing the vacuum masses and mixing angles by the corresponding parameters in matter

$$P_{\alpha\beta} = \sin^2 2\theta_m \sin^2 x_m, \quad x_m = \frac{\Delta m_m^2 L}{2E}.\tag{3.17}$$

The following points are worth mentioning regarding eq. (3.16):

- The vacuum result is reproduced for $A = 0$, as it should.
- Vacuum mixing is needed in order to get mixing in matter.
- To first order in x_m the matter effects cancel in the oscillation probability. To see this note that $x \sin 2\theta = x_m \sin 2\theta_m + O(x_m^3)$. Therefore, when approximating $\sin x_m \sim x_m$ eq. (3.17) reduces to the oscillation probability in vacuum, eq. (3.10).
- For $\Delta m^2 \cos 2\theta \gg |A|$, the matter effect is a small perturbation to the vacuum result.
- For $\Delta m^2 \cos 2\theta \ll |A|$, the neutrino mass is a small perturbation to the matter effect. In that case the oscillations are highly suppressed since the effective mixing angle is very small.
- For $\Delta m^2 \cos 2\theta = A$, the mixing is maximal, namely it is on resonance.

E. Non-uniform density

When the matter density is not constant there are further modifications to the oscillation formalism. Density variation results in changing the effective neutrino masses and their mixing angles. Then, the flavor composition of the neutrinos along their path is a function of the medium density profile.

At any point r on the neutrino path we define the derivative of the density

$$A'(r) = \frac{dA(r)}{dr}.\tag{3.18}$$

For constant density, $A' = 0$, the flavor conversion probability is controlled by the effective masses and mixing angles. For varying density, $A' \neq 0$, there are extra parameters that affect the flavor conversion probability. Most important is the adiabatic parameter

$$Q(r) = \frac{\Delta m^2 \sin^2 2\theta}{E \cos 2\theta} \frac{A(r)}{A'(r)}.\tag{3.19}$$

In the adiabatic limit, $Q \gg 1$, the density variation is slow. In this case the transition between effective mass eigenstates is highly suppressed, and the constant density formalism can be applied locally. In the non-adiabatic limit, $Q < 1$, the density variation is fast. Then, transition between effective mass eigenstates is possible, and the constant density formalism cannot be used. Both limits can be of interest in reality.

The best known example of the effect of the density variation is the MSW effect [11, 13]. It can account for a very efficient flavor conversion in the case of small mixing angle. Consider a two generation model where $m_2 > m_1$ with small vacuum mixing angle, $\theta \ll 1$. That is, in vacuum the muon neutrino is mainly ν_2 and the electron neutrino is mainly ν_1 . We consider neutrinos that are produced in the Sun core where the density is large. In particular, we are interested in the case where at the core of the Sun, $r = 0$, the matter induce effective electron neutrino mass-squared is much larger than the vacuum mass-squared difference, $A(0) \gg \Delta m^2$. Then, at $r = 0$ flavor eigenstates are almost pure effective mass eigenstates

$$\theta_m(r = 0) \rightarrow \pi/2, \quad \nu_e(r = 0) \approx \nu_2^m, \quad \nu_\mu(r = 0) \approx \nu_1^m. \quad (3.20)$$

(By writing $\nu_\alpha \approx \nu_i^m$ we mean that a very small rotation in flavor space is needed in order to move from the flavor eigenstate ν_α to the effective mass eigenstate ν_i^m .) In particular, the produced electron neutrino is almost a pure ν_2 . Also at the edge of the Sun, $r = R_\odot$, the flavor eigenstates are almost pure mass eigenstates

$$\theta_m(r = R_\odot) \rightarrow \theta \ll 1, \quad \nu_e(r = R_\odot) \approx \nu_1, \quad \nu_\mu(r = R_\odot) \approx \nu_2. \quad (3.21)$$

When the adiabatic limit applies, neutrinos propagate in the Sun as effective mass eigenstates. Since the neutrinos are produced as almost pure ν_2 , they leave the Sun as ν_2 . Since in vacuum ν_2 is almost a pure ν_μ , we learn that there is almost full conversion from ν_e to ν_μ . This phenomenon, which is called MSW resonance conversion, is demonstrated in fig. 2.

In the more general case, corrections to the adiabatic limit are taken into account. In particular, transitions between the effective mass eigenstates are important in the vicinity of the resonance. Such level crossing is described by the Landau-Zener probability, P_{LZ} . Then, the flavor conversion probability is given by the Parke formula [14]

$$P_{ee} = \frac{1}{2} [1 + (1 - 2P_{LZ}) \cos 2\theta_m \cos 2\theta], \quad (3.22)$$

where θ_m is the effective mixing angle at the production point. In this general case, the flavor transition probabilities become a rather involved function of the neutrino and medium parameters. It is this richness that makes the flavor composition of the solar neutrinos a complicated and not a monotonic function of their energies. As it is shown below this is important in order to be able to explain the solar neutrino data.

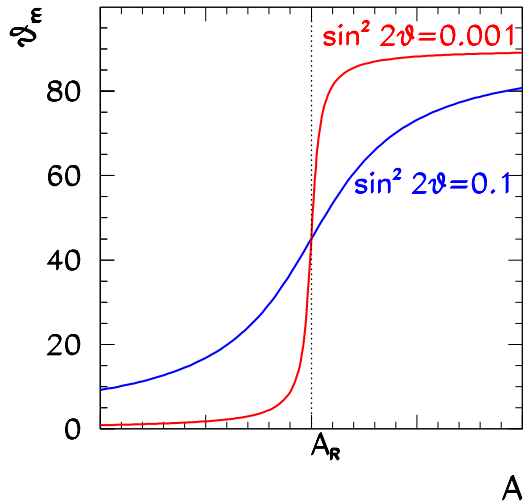


FIG. 2: A demonstration of an MSW resonance conversion. θ_m is the effective mixing angle in matter, A is the effective mass due to the matter effect defined in (3.15) and A_R is the resonance point. The neutrinos are produced at a region where $A > A_R$. They propagate as effective mass eigenstates, which is shown in the figure as solid lines. In the plot the effect is demonstrated for two different values of the vacuum mixing angles. (The plot is taken from [4].)

F. Neutrino oscillation experiments

Ideally, neutrino oscillation experiments measure the neutrino flavor transition probabilities as a function of the neutrino energies and their path. In practice, however, there are many experimental complications. The basic setup of any neutrino oscillation experiment is as follows: Neutrinos are produced and then propagate until few of them are detected at another location, far away from their production point. Therefore, in order to be able to probe the fundamental physics parameters we would like to know and control the following:

- The total flux, the flavor composition and the energy spectrum of the beam.
- The distance traveled by the neutrinos and the matter profile that they passed.
- The total flux, the flavor composition and the energy spectrum of the detected neutrinos.

In reality, it is impossible to know and control all of these parameters. Therefore, a lot of work is involved in order to get the maximum out of each experimental setup.

In general we distinguish between two kinds of experiments. Disappearance experiments search for reduction in the flux of a specific neutrino flavor

$$N[\nu_\alpha(L)] < N[\nu_\alpha(0)], \quad (3.23)$$

where $N[\nu_\alpha(L)]$ is the number of neutrinos of flavor α in the neutrino beam at distance L . This would imply

$$P_{\alpha\alpha}(L) < 1. \quad (3.24)$$

Appearance experiments, on the other hand, look for enhancement of a flux of a specific flavor

$$N[\nu_\beta(L)] > N[\nu_\beta(0)], \quad (3.25)$$

which would imply

$$P_{\alpha\beta}(L) > 0. \quad (3.26)$$

In particular, in many cases $N[\nu_\beta(0)] = 0$. Then, any observation of neutrinos with flavor β is an appearance signal.

Oscillation experiments are usually named after their production place and mechanism. In the following we discuss solar neutrinos, atmospheric neutrinos and terrestrial neutrinos.

IV. SOLAR NEUTRINOS

Solar neutrinos receive a lot of attention since there are indications for disappearance of electron neutrinos. These indications are collectively referred to as the solar neutrino problem or the solar neutrino anomaly. The best explanation for the solar neutrino problem is neutrino flavor oscillation.

The use of the words “problem” or “anomaly” should not worry us. They are used only to indicate the fact that solar neutrinos pose a problem to the SM. We think, however, that the SM is an effective theory of Nature, and thus, the fact that it faces problems is not surprising. Actually, we expect that neutrinos have masses and that they mix, and consequently, that the solar neutrino data cannot be explained by the SM.

A. Solar neutrinos production

Based on our understanding of stellar evolution we know that nuclear reactions fuel the Sun. Nuclear processes involve only the first generation of fermions and thus only electron neutrinos are generated in the Sun. Moreover, since the Sun is burn by fusion reactions it produces only neutrinos and not anti-neutrinos. The neutrino energies are relatively small, $E_\nu \lesssim 10$ MeV. Therefore, only disappearance experiments can be done; the neutrinos energies are too small to produce muons or taus in any target at rest.

There are many processes that produce solar neutrinos. The main reaction chain, which produces about 98.5% of the solar energy (and most of the solar neutrinos) is the pp cycle

$$4p \rightarrow {}^4\text{He} + 2e^+ + 2\nu_e + 2\gamma. \quad (4.1)$$

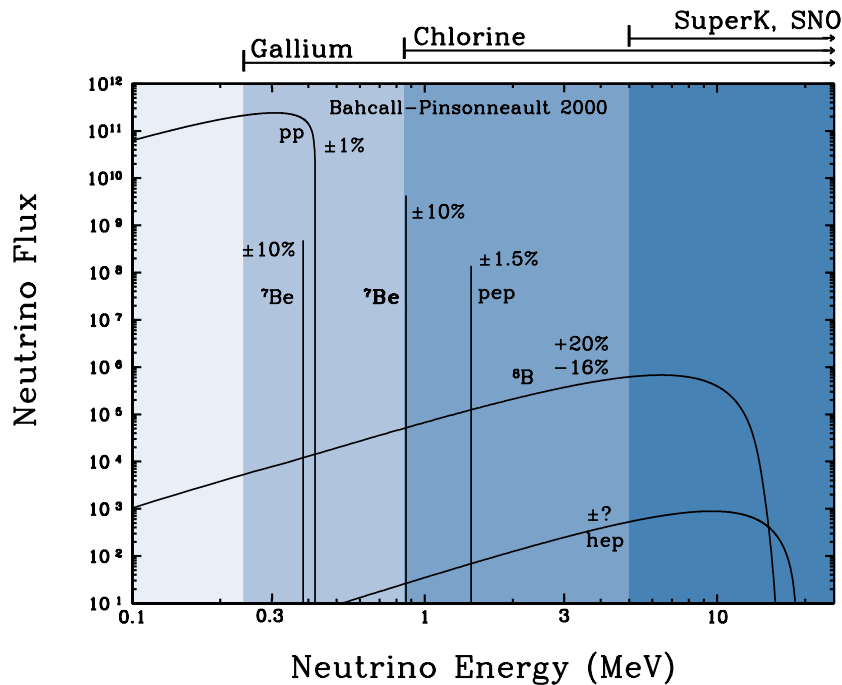


FIG. 3: The Bahcall and Pinsonneault 2000 solar model prediction of the neutrino flux as function of the neutrino energy. This figure was taken from [15], where many more details on solar neutrinos can be found.

The neutrinos emitted in this cycle have continuum spectrum which goes up to $E_\nu < 0.42$ MeV. Assuming that the Sun is in equilibrium, one can use its current luminosity to calculate the neutrino flux from the pp reaction chain.

The other nuclear reactions in the Sun are not very important for its luminosity, but they are important for neutrino physics. The difference originates from the fact that photons are thermalized almost immediately after they are produced. Neutrinos, on the other hand, do not interact in the Sun, and leave the Sun with their original energies. Several sub-dominant reactions produce neutrinos with energies above the threshold of the pp chain. Since it is easier to detect high energy neutrinos, in many cases the experimental signals consist only of neutrinos that were produced by sub-dominant reactions.

While the spectra of the different reactions are known, the sub-dominant reaction chains fluxes are not known in a model independent way. Solar models, namely, theoretical arguments, are used to obtain the total neutrino spectrum. As an example, the Bahcall and Pinsonneault 2000 (BP00) solar model prediction for the neutrino flux is given in fig. 3. Since solar models involve theoretical inputs, one would like to perform experiments where the interpretation of the data can be done with minimum dependence on a specific solar model.

B. Solar neutrinos propagation

Solar neutrinos are produced in the vicinity of the solar core. Then, they freely propagate out of the Sun and some of them travel to our detectors. During the night, neutrinos reach the detector after they have passed through the Earth. It is convenient to separate the solar neutrino propagation into three regions: inside the Sun, between the Sun and the Earth, and inside the Earth. We discuss each of these below.

As already mentioned before, matter effects in the Sun can be important for flavor conversion. To calculate these effects we need to know the matter profile in the Sun and the rates of the different reactions in the different parts of the Sun. While these parameters are roughly known, there are uncertainties in their values. Therefore, we have to count on solar models to provide the needed inputs.

The distance to the Sun is known to high precision. It varies by about 7% during the year. If vacuum oscillation is relevant to solar neutrinos then this distance variation can be used in order to get better control on the neutrino parameters.

During the night neutrinos pass through the Earth on their way to the detector, while during the day they do not. Therefore, the Earth matter effect, which shows up as a day-night difference of the detected neutrino flux, provides further sensitivity to the neutrino parameters. Moreover, depending on the location of the detector and the time of the year the neutrino may pass through both the Earth mantle and its core or only through the mantle. This is important since the matter density in these two regions is different, and therefore can affect the oscillations [16].

C. Solar neutrinos detections

There are three reactions that are used to detect solar neutrinos. The Charged Current (CC) interaction

$$\nu_e + n \rightarrow p + e^- , \tag{4.2}$$

where n is a neutron, can be used to detect only electron neutrinos. All the neutrinos can undergo Elastic Scattering (ES)

$$\nu_\ell + e^- \rightarrow \nu_\ell + e^- . \tag{4.3}$$

This reaction is mediated by neutral current Z exchange for all neutrino flavors. For electron neutrinos there is also contribution from a W exchange amplitude. Due to this difference, the elastic scattering cross section for electron neutrinos is about six times larger than for muon and tau neutrinos. Finally, the cross section for the Neutral Current (NC) interaction

$$\nu_\ell + n \rightarrow \nu_\ell + n , \tag{4.4}$$

is the same for all neutrino flavors (here n is a neutron).

When presenting results of neutrino oscillation experiment it is convenient to define

$$R = N_{obs}/N_{MC}, \quad (4.5)$$

such that N_{obs} is the number of detected neutrinos and N_{MC} is the number of events predicted from a solar model based Monte Carlo (MC) simulation assuming no flavor oscillation. For detectors that use neutral current reactions R should be one regardless if there are active neutrino flavor oscillations or not. For charged current and elastic scattering based detectors, however, $R = 1$ is expected only if there are no neutrino flavor oscillations, and $R < 1$ is expected if there are oscillations.

There are several solar neutrino experiments that use the above mentioned basic reactions. They have different experimental setups that use various reactions with different sensitivities and thresholds. Next we describe these experiments.

D. Chlorine: Homestake

The first detection of solar neutrinos was announced 35 years ago. The neutrinos were detected in the Homestake mine in South Dakota [17]. The experiment uses the



charged current interaction in order to capture the electron neutrinos.

We note the following points:

- The signal is extracted off-line. Namely, only integrated rates are measured. Therefore, no day-night and almost no spectral information are available. (The only information about the neutrino spectrum is that the energy of the neutrino is above the threshold.)
- The energy threshold is 0.814 MeV. Therefore, the experiment is sensitive mainly to the ${}^7\text{Be}$ and ${}^8\text{B}$ neutrinos. pp neutrinos cannot be detected in this experiment.
- After many years of data collection the published result is [18]

$$R \approx 0.3. \quad (4.7)$$

Of course, in order to perform a fit to the neutrino parameters the above crude approximation should not be used. Yet, quoting the order of magnitude, as we did in eq. (4.7) is sufficient to understand the main ingredients of the solar neutrino problem.

The fact that the Homestake experiment found $R < 1$ was the first indication for solar electron neutrino disappearance. This result gave the motivation to build different types of detectors in order to further study the solar neutrinos.

E. Gallium: SAGE, GALLEX and GNO

The Homestake experiment had relatively high threshold. The SAGE, GALLEX [19] and GNO [20] Gallium experiments were built in order to detect neutrinos with much smaller energies. In particular, their threshold is low enough to detect pp neutrinos. In the Gallium experiments the neutrinos are detected using the



charged current reaction.

We note the following points:

- Like the Chlorine experiment, the signal is extracted off-line. Thus, also here no day-night and spectral information are available.
- The energy threshold is 0.233 MeV. Thus, Gallium detectors are sensitive to pp neutrinos. The ${}^7\text{Be}$ and ${}^8\text{B}$ neutrinos also contribute significantly to the neutrino signal. Therefore, the total predicted flux is not solar model independent.
- Combining the results of the three experiments, one obtains

$$R \approx 0.6. \quad (4.9)$$

We learn that like in the Chlorine experiment, also here, the number of observed electron neutrinos is less than predicted. Moreover, the measured R is different for the two type of experiments. Since these two types are sensitive to different energy ranges, this fact indicates that the electron neutrino flux reduction must be energy dependent.

F. Water Cerenkov: Kamiokande and SuperKamiokande

Both the Chlorine and Gallium experiments extract their signal off-line. The Kamiokande and SuperKamiokande [21] water Cerenkov detectors can extract their signal on-line. Therefore, in these experiments day-night and spectral information can be extracted. The price to pay is that the energy threshold is much higher compared to the thresholds of the Chlorine and Gallium experiments.

In the water Cerenkov detectors the neutrinos are detected by elastic scattering of the neutrinos off the electrons in the water

$$\nu_\alpha + e^- \rightarrow \nu_\alpha + e^- . \quad (4.10)$$

We note the following points:

- Since the detection is done on-line, the time of each event is known, and also some information about the direction and energy of the neutrino in each event can be extracted. These features enable the experiments to clearly show that the detected neutrinos are coming from the Sun.
- The water Cerenkov detectors threshold is about 6 MeV. Thus, the Kamiokande and SuperKamiokande experiments are sensitive mainly to ^8B neutrinos.
- Since elastic scattering is used for the detection, all neutrino flavors contribute to the signal. This fact is important if there are active flavor oscillations. Then, the converted neutrinos also contribute to the signal. This is in contrast to detectors that use charged current interactions where only electron neutrinos generate the signal.
- The integrated suppression is found to be

$$R \approx 0.5. \tag{4.11}$$

Spectrum and day-night information were also reported.

We learn again that there is an energy dependent suppression of the electron neutrino flux.

G. Heavy Water: SNO

We already mentioned that neutrino flavor conversion is the most plausible explanation to the observed energy dependent electron neutrino flux suppression. Thus, it is interesting to measure solar neutrinos using neutral current reactions since in that case all neutrino flavors contribute with the same strength. Namely, neutral current based experiments measure the solar neutrino flux independent of whether there are active flavor oscillations or not.

The SNO detector [22] was built for this purpose. Its apparatus contains an inner tank filled with heavy water and an outer tank filled with regular water. Neutrino can be detected by all the three basic reaction types

$$\begin{aligned}
\text{CC}(E_{th} = 2.23 \text{ MeV}) : & \quad \nu_e + {}^2\text{H} \rightarrow p + p + e^-, \\
\text{ES}(E_{th} \sim 6 \text{ MeV}) : & \quad \nu_\alpha + e^- \rightarrow \nu_\alpha + e^-, \\
\text{NC}(E_{th} \sim 6 \text{ MeV}) : & \quad \nu_\alpha + {}^2\text{H} \rightarrow n + p + \nu_\alpha,
\end{aligned} \tag{4.12}$$

where E_{th} is the threshold energy. Note that the presence of Deuterium (${}^2\text{H}$) in the heavy water is crucial for the charged current and neutral current measurements.

Note the following points:

- The signal is extracted on-line. Thus day-night and spectrum information is available.

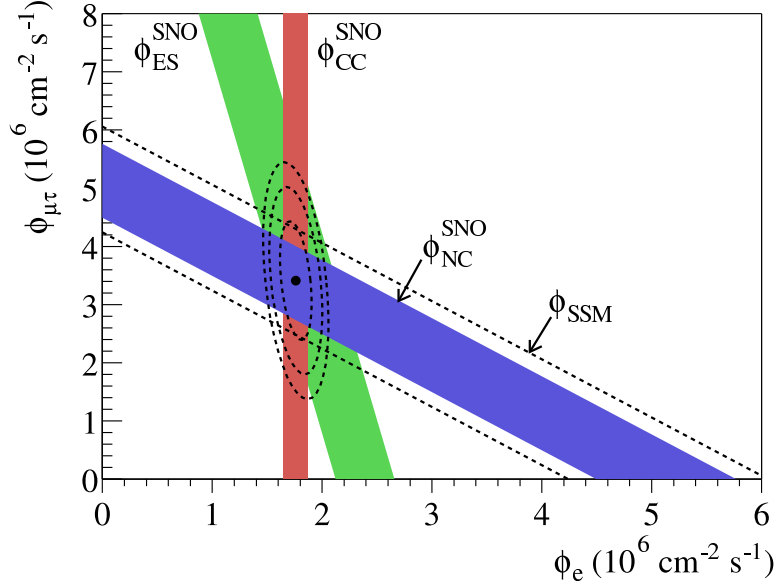


FIG. 4: The SNO data is plotted as three independent measurements of the muon or tau neutrino flux ($\phi_{\mu\tau}$) as a function of the electron neutrino flux (ϕ_e). The three bands represent the neutral current, charged current and elastic scattering based measurements. The dotted line is the BP00 solar model prediction for the neutrino flux. It is plotted only in conjunction with the neutral current measurement since only this measurement is insensitive to electron to muon or tau flavor conversion. (This plot is taken from [23].)

- We define the ratios

$$R_E \equiv \frac{R_{CC}}{R_{ES}}, \quad R_N \equiv \frac{R_{CC}}{R_{NC}}, \quad (4.13)$$

where R_{CC} (R_{ES} , R_{NC}) is the ratio between the observed number of charged current (elastic scattering, neutral current) events and the predicted number assuming no oscillation. Extracting R_E and R_N has several advantages. First, many systematic uncertainties cancel in their measurements. Second, their predicted values are almost solar model independent and depend only on the neutrino parameters. In particular, $R_E \neq 1$ or $R_N \neq 1$ can occur only if electron neutrinos are converted to muon or tau neutrinos.

- SNO found $R_E \neq 1$ and $R_N \neq 1$. This result confirms the existence of ν_μ or ν_τ component in the solar neutrino flux at 5.3σ . In addition, the BP00 solar model prediction is confirmed by the neutral current measurement. The SNO result [23] is illustrated in fig. 4.

H. Solar neutrinos: fits

The general picture emerging by combining all the solar neutrino data is as follows. All charged current and elastic scattering based measurements found less events than predicted for massless neutrinos. This suppression is energy dependent. The BP00 solar model prediction for the neutral current based measurement, which holds also if there are active neutrino flavor conversions, was confirmed by SNO.

The first and most robust conclusion is that the SM, which predicts massless neutrinos, fails to accommodate the data. While there are several exotic explanations that may be able to explain the data [24], the simplest and most plausible one is that of active neutrino flavor oscillation

$$\nu_e \rightarrow \nu_x, \quad x = \mu, \tau. \quad (4.14)$$

In that case, experiments that use reactions that are flavor dependent, namely charged current interactions and elastic scattering, are expected to detect fewer events than anticipated. On the other hand, experiments that use neutral current interactions, which are flavor blind, should not observe such reduction. Indeed, this is what the data shows.

Assuming that the neutrinos are massive, the data can be used to determine the neutrino masses and mixing angles. While three flavor oscillation fits are available [25], it is a good approximation to fit the data assuming only two neutrino mixing. An example of such fit is shown in fig. 5. (Recent fits can be found in [25]. Note, however, that whenever new data is published, new fits are performed and published usually within days.) The regions where a good fit is found are indicated in the figure. The best fit is obtained in the Large Mixing Angle (LMA) region. The recent SNO data actually exclude the Small Mixing Angle (SMA) region. The LOW and the Vacuum Oscillation (VO) regions, are still allowed by all solar data. They are excluded, however, by the recent KamLAND result, see below.

To conclude, there are strong indications for active $\nu_e \rightarrow \nu_x$ oscillation. This conclusion is robust since it has practically no dependence on the solar model. The best fit to the neutrino parameters is in the LMA region with

$$\Delta m^2 = 6 \times 10^{-5} \text{ eV}^2, \quad \tan^2 \theta = 0.4. \quad (4.15)$$

Future data and new experiments will teach us more about solar neutrinos. Besides having more statistics, future experiments will measure observables where we have only very little information at present. In particular, we expect to have more information about the day-night effect and the low energy neutrino spectrum.

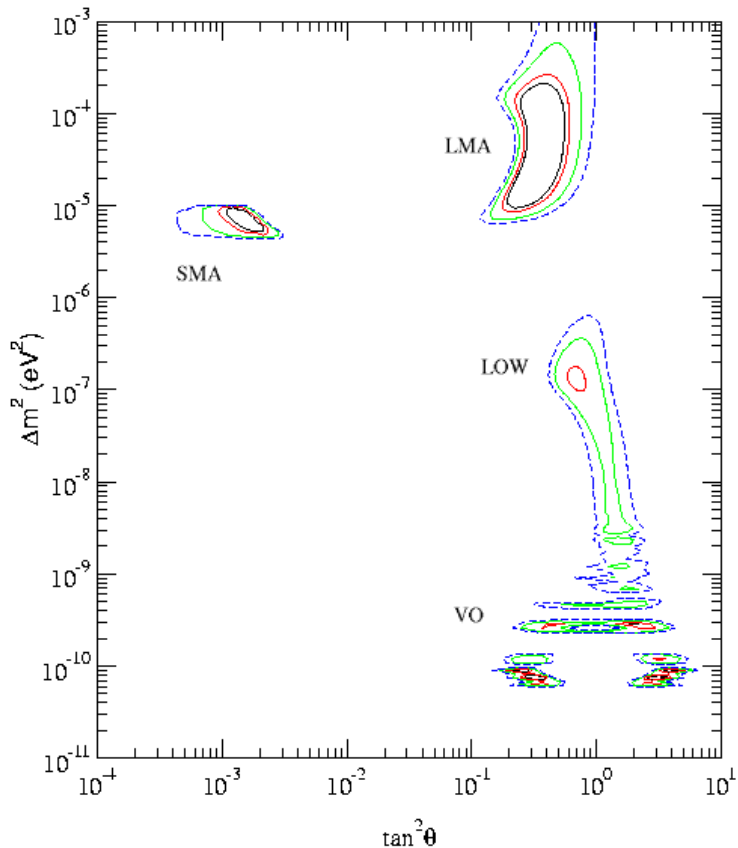


FIG. 5: An example of a neutrino parameters fit to some solar neutrino data. The names of the regions where good fit is found are indicated in the figure. Note that by now this fit is outdated, and it is shown here for illustration only. (This plot is based on a plot taken from [26].)

V. ATMOSPHERIC NEUTRINOS

In the reaction chain initiated by cosmic ray collisions off nuclei in the upper atmosphere neutrinos are produced. These neutrinos are searched for by atmospheric neutrinos experiments. There are indications for muon neutrinos disappearance. These indications are called the atmospheric neutrino problem or the atmospheric neutrino anomaly. The likely explanation of this phenomenon is active neutrino oscillation.

A. Atmospheric neutrino production

Cosmic ray collisions off nuclei in the upper atmosphere produce hadrons, mainly pions. In their decay chain

$$\pi^+ \rightarrow \mu^+ \nu_\mu, \quad \mu^+ \rightarrow e^+ \nu_e \bar{\nu}_\mu, \quad (5.1)$$

(and the charge conjugated decay chain) neutrinos are produced. Note that almost exclusively electron and muon neutrinos are produced. Based on (5.1) we expect

$$N(\nu_\mu)/N(\nu_e) \approx 2, \quad (5.2)$$

where $N(\nu_\ell)$ is the number of neutrinos of flavor ℓ . There are corrections to this prediction. Other mesons, mainly kaons, are also produced by cosmic rays. Their decay chains produce different neutrino flavor ratio. Another effect is that at high energies the muon lifetime in the lab frame is much longer than in its rest frame. In fact, it is long enough such that not all the muons decay before they arrive to the detector. All in all, the neutrino production rates and spectra are known to an accuracy of about 20%. The ratio $N(\nu_\mu)/N(\nu_e)$ is known better, to an accuracy of about 5%.

The atmospheric neutrino energies are relatively large, $E_\nu \gtrsim 100$ MeV. Therefore, both disappearance and appearance experiments are possible. In particular, since the initial tau neutrino flux is tiny, searching for tau appearance is an attractive option.

B. Atmospheric neutrino propagation

Since neutrinos are produced isotropically in the upper atmosphere, they reach the detector from all directions. The neutrino zenith angle in the detector is correlated with the distance it traveled. Neutrinos with small zenith angle, namely those coming from above, travel short distances (of order 10^2 km). Neutrinos with large zenith angle, namely those coming from below, are neutrinos that cross the Earth and travel much longer distances (of order 10^4 km). Since the production is isotropic, the neutrino flux in the detector is expected to be isotropic in the absence of oscillation. (There are small known corrections due to geo-magnetic effects.)

Matter effects can be important for neutrinos that cross the Earth. Oscillations that involve electron neutrinos or oscillations between active and sterile neutrinos are modified in the presence of matter. In contrast, the matter has almost no effect on $\nu_\mu \rightarrow \nu_\tau$ oscillation.

C. Atmospheric neutrino detection

There are two types of atmospheric neutrino detectors. The water Cerenkov detectors, IMB, Kamiokande and SuperKamiokande [21], use large tanks of water as targets. The water is surrounded by photomultipliers which detect the Cerenkov light emitted by charged leptons that are produced in charged current interactions between the neutrinos and the

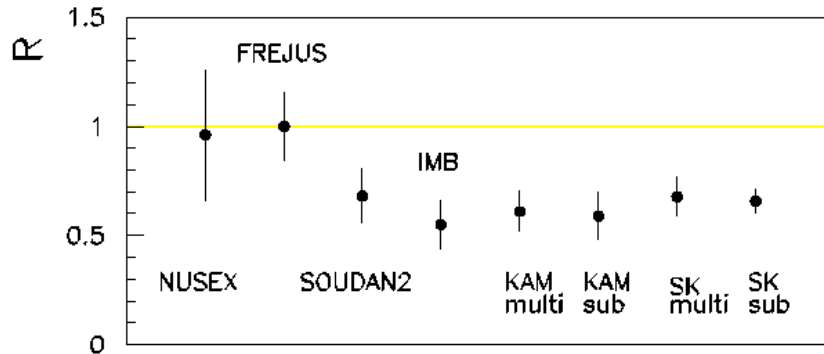


FIG. 6: Summary of the experimental measurements of R defined in eq. (5.3). (This plot is taken from [4].)

water. Compared to electrons, muons are likely to create sharper Cerenkov rings. Thus, the shape of the ring helps in determining the flavor of the incoming neutrino. Iron calorimeter detectors are based on a set of layers of iron which act as a target, and some tracing elements that are used to reconstruct muon tracks or showers produced by electrons.

Both water Cerenkov and Iron calorimeter detectors identify the neutrino flavor via its charged current interactions. They have some ability to look for neutral current interactions. Information on the neutrino energy and direction can also be extracted by both methods.

D. Atmospheric neutrino data

All atmospheric neutrino experiments measure the double ratio

$$R = \frac{N_{obs}^{\mu}/N_{obs}^e}{N_{MC}^{\mu}/N_{MC}^e}, \quad (5.3)$$

where N_{MC}^{ℓ} is the expected number of flavor ℓ type events and N_{obs}^{ℓ} are the observed ones. The advantage of using this double ratio is that many systematic and theoretical errors cancel in this ratio. Almost all of the experiments found $R < 1$; see fig. 6.

The observation of $R < 1$ can be explained by muon neutrino disappearance, electron neutrino appearance, or both. The SuperKamiokande experiment also measured the zenith angle dependence of the neutrino flux. The data indicate that the preferred explanation is that of muon neutrino disappearance. For example, fig. 7 shows that the low energy ν_e flux agrees while the ν_{μ} flux disagrees with the MC prediction.

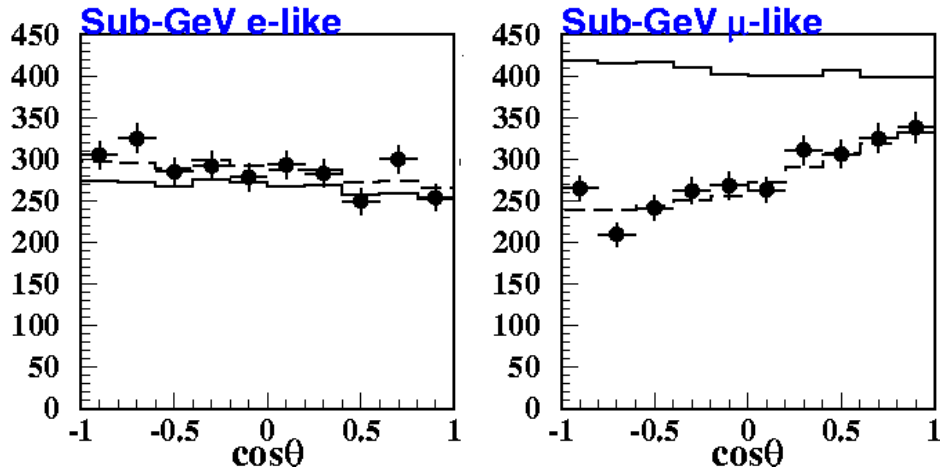


FIG. 7: The low energy electron and muon neutrino fluxes compared to the MC predictions as observed by SuperKamiokande. The solid lines are the expected fluxes assuming no oscillations. The dashed lines are the best fits to neutrino oscillation. The solid circles are the data points. (This plot is taken from [27].)

E. The atmospheric neutrino problem

The zenith angle dependence of the muon neutrino flux as well as $R < 1$ cannot be explained with SM massless neutrinos. This is called the atmospheric neutrino anomaly. In order to explain its disappearance of muon neutrinos is needed. While there are several exotic explanations [24], the most attractive explanation is active neutrino flavor oscillation. In particular, the best fit is achieved for $\nu_\mu \rightarrow \nu_\tau$ oscillation with

$$\Delta m^2 = 2.6 \times 10^{-3} \text{ eV}^2, \quad \sin^2 2\theta = 0.97. \quad (5.4)$$

The hypothesis of neutrino oscillation can be further tested. First, terrestrial long baseline experiments probe the same region of parameter space as the atmospheric neutrino experiments. Indeed, as discussed in more detail below, the recent K2K long baseline experiment results agree with the atmospheric neutrino data. Second, search for tau appearance in the atmospheric neutrino data is also possible. The SuperKamiokande experiment found such indications [28], but they are not yet convincing.

VI. TERRESTRIAL NEUTRINOS

One disadvantage of solar and atmospheric neutrino measurements is that since the neutrinos are not produced on Earth, there is no control over the neutrino source. Neutrinos

from accelerators and nuclear reactors have the advantage that their source is known. That is, we know to high accuracy the initial neutrino flux, the energy spectrum and the flavor composition of the neutrino source. Moreover, in some cases these parameters can be tuned in order to maximize the experimental sensitivity.

The main advantage of solar and atmospheric neutrinos is that they are sensitive to very small Δm^2 . That is, their sensitivity is much better compared to most terrestrial neutrino experiments. Therefore, it is not surprising that most terrestrial neutrino experiments did not find disappearance or appearance signals. Their data was used to set bounds on the neutrino parameters. There are, however, some exceptions. The sensitivity of the K2K [29] and KamLAND [30] experiments are similar to those of, respectively, the atmospheric and solar neutrino experiments. Recently, positive disappearance signals were found in these two terrestrial experiments. The situation is different with regard to the LSND [31] experiment. In that case there is a claim for an appearance signal. This signal can only be explained with neutrino masses that are much larger compared to the masses deduced from the solar and atmospheric neutrino data. Next we describe these three experiments and their results.

A. K2K

In order for accelerator neutrinos to be sensitive to the same range of parameter space as the atmospheric neutrino experiments, long baseline, of order 10^3 km, is needed. In such long baseline experiments it is possible to search for ν_μ disappearance or ν_τ appearance. In these experiments a neutrino beam from an accelerator is aimed at a detector located far away. The first operating long baseline experiment is the K2K experiment. It uses an almost pure ν_μ beam that is generated at KEK and is detected at SuperKamiokande, which is about 250 km away.

Recently, the K2K experiment announced their first result [32]. They observed 56 muon neutrino events with an expectation of about 80. The ν_μ disappearance can be explained by $\nu_\mu \rightarrow \nu_x$ flavor oscillation. The best fit is found for the following values

$$\Delta m^2 = 2.8 \times 10^{-3} \text{ eV}^2, \quad \sin^2 2\theta = 1.0. \quad (6.1)$$

These values of the neutrino parameters are very close to those indicated by the atmospheric neutrino data, see eq. (5.4). The statistical significance of the K2K oscillation signal is smaller than the atmospheric neutrino ones. The importance of the K2K result lies in the fact that it provides an independent test of the atmospheric neutrino parameter space.

B. KamLAND

Reactor neutrinos have much smaller energies compared to neutrinos produced at accelerator. Thus, long baseline reactor experiments are sensitive to smaller values of Δm^2 . Another important difference is that reactors generate only electron anti-neutrinos, while accelerators produce mainly muon neutrinos. Thus, reactor experiments can be used to provide independent probes of the solar neutrino parameter space.

The KamLAND experiment is placed in the Kamioka mine in Japan. This site is located at an average distance of about 180 km from several large Japanese nuclear power stations. The initial fluxes and spectra of the $\bar{\nu}_e$ emitted in each reactor are known to a good accuracy, since they are related to the power that is generated in each reactor. Thus, measurement of the total flux and energy spectrum of the $\bar{\nu}_e$ at KamLAND can be used to search for disappearance. This is particularly interesting since the KamLAND setup is such that it is sensitive to the region of the parameter space indicated by the LMA solution to the solar neutrino anomaly.

Recently, the KamLAND experiment announced their first result [33]. They found

$$\frac{N_{obs}}{N_{MC}} = 0.611 \pm 0.085 \pm 0.041 \quad (6.2)$$

where N_{obs} is the number of observed events and N_{MC} is the expected number. This result can be explained by $\bar{\nu}_e \rightarrow \bar{\nu}_x$ neutrino flavor oscillation with the best fit at

$$\Delta m^2 = 6.9 \times 10^{-5} \text{ eV}^2, \quad \sin^2 2\theta = 1.0. \quad (6.3)$$

These values are very close to the ones indicated by the solar neutrino data, see eq. (4.15).

The importance of this result is twofold. First, it provides a completely solar model independent test for the neutrino oscillation solutions of the solar neutrino problem. Moreover, it discriminates between the different possible solutions, pointing at the LMA as the favorable one.

C. LSND

The set up of the LSND experiment [31] is as follows. Neutrinos are produced by sending protons on a fixed target that generates pions. Almost all the negatively charged pions are absorbed in the target before they decay. The neutrinos are produced via

$$\pi^+ \rightarrow \mu^+ \nu_\mu, \quad \mu^+ \rightarrow e^+ \nu_e \bar{\nu}_\mu. \quad (6.4)$$

Then, the neutrinos travel for about 30 meter to the detector. Since the beam contains ν_μ , ν_e and $\bar{\nu}_\mu$, with negligible fraction of $\bar{\nu}_e$, it best to search for $\bar{\nu}_\mu \rightarrow \bar{\nu}_e$ appearance.

The LSND collaboration announced a 3.3σ indication for $\bar{\nu}_e$ appearance

$$P(\bar{\nu}_\mu \rightarrow \bar{\nu}_e) = (2.64 \pm 0.67 \pm 0.45) \times 10^{-3}. \quad (6.5)$$

This result can be explained with $\bar{\nu}_\mu \rightarrow \bar{\nu}_e$ oscillation where the best fit is achieved for

$$\Delta m^2 = 1.2 \text{ eV}^2, \quad \sin^2 2\theta = 0.003. \quad (6.6)$$

Note that the value of Δm^2 in (6.6) is much larger than the values indicated by the solar and atmospheric neutrino data.

The LSND indications for neutrino masses are not as strong as the solar and atmospheric neutrino ones. First, the statistical significance of the LSND signal is rather low (traditionally, only a 5σ effect is called a discovery). Second, the LSND signal still needs an independent confirmation. The Karmen experiment [34], which has a setting similar to LSND, but with a shorter baseline, $L \approx 17$ meter, did not find an appearance signal. Soon, the MiniBooNE experiment [35] will be able to clarify the situation.

VII. THEORETICAL IMPLICATIONS

As we have seen, there are solid experimental indications for neutrino masses. The most important implication of these results is also the most simple one: the SM is not the complete picture of Nature. Namely, there are experimental indications that the SM is only an effective low energy description of Nature.

There are basically two ways to extend the SM. One way is to assume that there is new physics only at a very high scale, much above the weak scale. Then, neutrino masses can be accounted for by the seesaw mechanism. Alternatively, one can think about weak scale new physics. Neutrino masses that are generated by such new physics are, in general, too large and some mechanism is required in order to explain the smallness of the neutrino masses. In the following we concentrate on the former option.

A. Two neutrino mixing

We start by considering only one type of results at a time. Namely, we draw conclusions from the solar and KamLAND data or from the atmospheric and K2K data. In that case there is one theoretical challenge imposed by the data: how to generate neutrino masses at the right scale?

The atmospheric neutrinos and K2K results indicate $\nu_\mu \rightarrow \nu_\tau$ oscillation with

$$\Delta m_{\text{AN}}^2 \sim \text{few} \times 10^{-3} \text{ eV}^2. \quad (7.1)$$

The solar neutrinos and KamLAND results indicate $\nu_e \rightarrow \nu_{\mu,\tau}$ oscillation with

$$\Delta m_{\text{SN}}^2 \sim 10^{-4} \text{ eV}^2. \quad (7.2)$$

We use (2.9) in order to obtain the scale of the new physics that is responsible for neutrino masses

$$m_\nu = \frac{m_D^2}{M} \quad \Longrightarrow \quad M = \frac{m_D^2}{m_\nu}. \quad (7.3)$$

In order to find the high energy scale, M , we need to know m_ν and m_D . The most likely situation is that the neutrinos are not degenerate

$$\frac{\Delta m_{ij}^2}{m_i^2 + m_j^2} \sim 1. \quad (7.4)$$

Then, we use $m_\nu \sim \sqrt{\Delta m^2}$. In general, the Dirac masses are of the order of the weak scale times dimensionless couplings. The problem is that we do not know the value of these couplings. In the following we make two plausible choices for their values. Motivated by $SO(10)$ GUT theories, we assume that these couplings are of order of the up type quark Yukawa couplings. In particular, for the heaviest neutrino, the coupling is of the order of the top Yukawa coupling. Another plausible choice is to use the charged lepton Yukawa couplings as a guide to the neutrino ones.

Considering atmospheric neutrino and K2K data we use $m_\nu \sim \text{few} \times 10^{-2} \text{ eV}$ and get

$$\begin{aligned} m_D \sim m_t & \quad \Longrightarrow \quad M \sim 10^{16} \text{ GeV}, \\ m_D \sim m_\tau & \quad \Longrightarrow \quad M \sim 10^{11} \text{ GeV}. \end{aligned} \quad (7.5)$$

If instead we use $m_\nu \sim 10^{-2} \text{ eV}$ as indicated by solar neutrinos and KamLAND data, we obtain

$$\begin{aligned} m_D \sim m_t & \quad \Longrightarrow \quad M \sim \text{few} \times 10^{16} \text{ GeV}, \\ m_D \sim m_\tau & \quad \Longrightarrow \quad M \sim 10^{12} \text{ GeV}. \end{aligned} \quad (7.6)$$

We emphasize the following points:

- Both eqs. (7.5) and (7.6) imply that there exists a new scale between the weak scale and $M_{\text{Pl}} \sim 10^{19} \text{ GeV}$.
- The values obtained assuming $m_D \sim m_t$ in both eqs. (7.5) and (7.6) are very close to the GUT scale, $M_{\text{GUT}} \sim 3 \times 10^{16} \text{ GeV}$. Therefore, we can say that neutrino masses are indications in favor of unification.
- In several new physics models, a new scale, usually called the intermediate scale, $M_{\text{Int}} \sim \sqrt{m_W M_{\text{Pl}}} \sim 10^{11} \text{ GeV}$, is introduced. For example, supersymmetry breaking has to occur at this scale if it is mediated via Planck scale physics to the observable sector. The values obtained assuming $m_D \sim m_\tau$ in both eqs. (7.5) and (7.6) are very close to M_{Int} . This could be an indication that neutrino masses are also generated by such models.

B. Three neutrino mixing

When we combine the solar, KamLAND, atmospheric and K2K data, we have to consider the full three flavor mixing. There are three mass differences that control the oscillations. They are subject to one constraint

$$\Delta m_{12}^2 + \Delta m_{23}^2 + \Delta m_{31}^2 = 0. \quad (7.7)$$

The data indicates that the mass-squared differences are hierarchical, $|\Delta m_{12}^2| \ll |\Delta m_{23}^2|$. This implies that $|\Delta m_{23}^2| \approx |\Delta m_{31}^2|$, and therefore, that there are only two different oscillation periods.

There are three mixing angles. Solar neutrino oscillations depend mainly on θ_{12} and atmospheric neutrino oscillations depend mainly on θ_{23} . The third angle, θ_{13} , is known to be small, mainly from terrestrial experiments (see, for example, [4] for details). Thus, the oscillation phenomena are described by two mass-squared differences and three mixing angles

$$\begin{aligned} \Delta m_{12}^2 &\sim 10^{-4} \text{ eV}^2, & \Delta m_{23}^2 &\sim \text{few} \times 10^{-3} \text{ eV}^2, \\ \theta_{12} &\sim 1, & \theta_{23} &\sim 1, & \theta_{13} &\lesssim 0.2. \end{aligned} \quad (7.8)$$

As before, we assume that the neutrinos are not degenerate. Then, we learn from (7.8) that the neutrino masses are somewhat hierarchical with two large and one small mixing angles.

The theoretical challenge imposed by considering three neutrino flavor mixing is to explain the flavor structure of (7.8). There are basically two approaches to do so. One is called neutrino anarchy [36]. It assumes that there are no parametrically small numbers. The two apparently small numbers in the neutrino sector

$$\frac{m_2}{m_3} \sim \frac{1}{5}, \quad \theta_{13} \sim \frac{1}{5}, \quad (7.9)$$

are assumed to be accidentally small. That is, numbers of order five are considered natural. Therefore, this mechanism predicts that θ_{13} is close to its current upper bound. Consequently, it also predicts that CP violating observables, which are proportional to the product of all the mixing angles and the neutrino mass-squared differences, should also be close to their current upper bounds.

The other option to explain (7.8) is to assume that there is an underlying broken flavor symmetry that controls the neutrino sector parameters. Such a symmetry is often assumed in order to explain the quark sector flavor parameters. Within this framework it is assumed that there is one small parameter, ϵ , such that all the small parameters of the theory are functions of it. In particular,

$$\frac{m_2}{m_3} \sim \epsilon^n \ll 1, \quad \theta_{13} \sim \epsilon^m \ll 1, \quad (7.10)$$

where n and m are some positive integers. In that case we often refer to observables like m_2/m_3 and θ_{13} as parametrically small numbers.

While flavor symmetries can explain the observed hierarchies in the quark sector, it is not straightforward to extend the treatment to the neutrinos. The main reason is that in general large mixing angles come without mass hierarchies and vice versa. Explicitly, we consider the two generation case. The neutrino mass matrix is

$$m = \begin{pmatrix} a & b \\ b & c \end{pmatrix}, \quad (7.11)$$

and we distinguish the following three cases

- $a \gg b, c \implies \sin^2 \theta \ll 1, \quad m_1/m_2 \ll 1.$
- $a, b, c \sim 1, \quad \det(m) \sim 1 \implies \sin^2 \theta \sim 1, \quad m_1/m_2 \sim 1.$
- $a, b, c \sim 1, \quad \det(m) \ll 1 \implies \sin^2 \theta \sim 1, \quad m_1/m_2 \ll 1.$

We learn that in order to have large mixing with mass hierarchy the determinant of the mass matrix must be much smaller than the typical value of its entries (to the appropriate power). This is not a common situation in flavor models. In particular, this is not the case in the quark sector.

C. Four neutrino mixing

While the LSND data cannot be considered as a solid indication for neutrino masses, one may like to try to accommodate it as well. In that case the situation become much more complicated. The reason is that three different mass-squared differences are needed

$$\Delta m_{\text{SN}}^2 \sim 10^{-4} \text{ eV}^2, \quad \Delta m_{\text{AN}}^2 \sim \text{few} \times 10^{-3} \text{ eV}^2, \quad \Delta m_{\text{LSND}}^2 \sim 1 \text{ eV}^2. \quad (7.12)$$

With three neutrinos, however, the constraint (7.7) implies that there are at most two different scales. Therefore, at least four neutrinos are needed in order to accommodate all of these results. Experimentally we know that there are only three active neutrinos, and thus we need at least one additional light sterile neutrino field.

There are two theoretical challenges: First, a sterile neutrino, by definition, is a fermion that is a singlet under the SM gauge group. As such, it can acquire very large mass since there is no gauge symmetry that forbids it. Thus, a sterile neutrino naturally has very large mass. There are, however, several ideas that produce naturally light sterile states [37].

Even if there are light sterile states, complicated patterns of masses and mixing angles are required in order to accommodate all the data. In fact, even adding a sterile state does not help in obtaining a good fit to the data [38]. In the following we do not address the four neutrino mixing any further.

VIII. MODELS FOR NEUTRINO MASSES

As we saw there are three different kinds of theoretical challenges imposed by the neutrino data. Considering separately the solar and the atmospheric neutrino data, the challenge is to generate neutrino masses at the right scale. Combining them, we would like to find ways to generate the flavor structure, in particular, to explain mass hierarchy with large mixing. In order to accommodate also the LSND result, we should find a mechanism that generates light sterile neutrinos, and construct even more complicated flavor structure.

The simplest way to generate neutrino masses is the seesaw mechanism. It is particularly attractive when it appears in models that are well motivated because they address various theoretical puzzles. Below we describe two models where neutrino masses are generated as one aspect of a model. (See [2, 4] for more examples.)

A. Grand Unified Theories (GUTs)

There are several supporting evidences for supersymmetric grand unification. First, in the minimal supersymmetric SM (MSSM) the three gauge couplings unify at one point at a scale of

$$\Lambda_{\text{GUT}} \sim 3 \times 10^{16} \text{ GeV}. \quad (8.1)$$

Second, one generation of SM fermions fits into two $SU(5)$ multiplets and into one multiplet for higher rank GUT groups. Neutrino physics provide further support for GUT, particularly, for GUTs that are based on $SO(10)$ (or higher rank) gauge group. Next we describe two of the facts that make $SO(10)$ GUTs attractive from the point of view of neutrino physics.

The 15 degrees of freedom of one SM fermion generation fall into a **16** of $SO(10)$. The one extra degree of freedom is a SM singlet. Thus, it can serve as a right handed neutrino field. Once $SO(10)$ is broken, this singlet becomes massive. Consequently, the SM active neutrinos acquire small masses via the seesaw mechanism. Namely, neutrino masses are predictions of $SO(10)$ GUT theories.

$SO(10)$ also predicts the rough scale of the neutrino masses. To see it recall that $SO(10)$ relates the up type quark masses to the Dirac masses of the neutrinos. In particular, the Dirac mass of the heaviest neutrino is of the order of the mass of the top quark. The Majorana mass of the singlet is expected to be of the order of the GUT breaking scale, $M_N = \lambda \Lambda_{\text{GUT}}$ where λ is an unknown dimensionless number. Then, the seesaw generated mass of the heaviest active neutrino is of the order of

$$m_3 \sim \frac{m_t^2}{M_N} \sim \frac{10^{-3} \text{ eV}}{\lambda}. \quad (8.2)$$

For $\lambda \sim O(10^{-1})$ it is the mass scale that was found by solar neutrinos. Somewhat smaller λ is needed in order to get the scale that is relevant for atmospheric neutrino oscillation. Generally, it is fair to say that $SO(10)$ based theories predict neutrino masses in accordance with the experimental findings.

B. Flavor physics

The most puzzling features of the SM fermion parameters are their smallness and the hierarchies between them. These features suggest that there is a more fundamental theory where the hierarchies are generated in a natural way. Generally, a broken horizontal symmetry is invoked. (By horizontal symmetry we refer to a symmetry that distinguishes between the three SM generations.)

We demonstrate this broken flavor symmetry idea by working in the framework of a supersymmetric $U(1)_H$ horizontal symmetry [39]. We assume that the low energy spectrum consists of the fields of the MSSM. Each of the supermultiplets carries a charge under $U(1)_H$. The horizontal symmetry is explicitly broken by a small parameter λ to which we attribute a charge -1 . Then, the following selection rules apply: Terms in the superpotential that carry a charge $n \geq 0$ under H are suppressed by $O(\lambda^n)$, while those with $n < 0$ are forbidden due to the holomorphy of the superpotential.

Explicitly, the lepton parameters arise from the Yukawa terms

$$Y_{ij}L_iE_jH_d + \frac{Z_{ij}}{M}L_iL_jH_uH_u. \quad (8.3)$$

Here L_i (E_i) are the lepton doublet (singlet) superfields, H_u (H_d) is the up type (down type) Higgs superfields, Y_{ij} is a generic complex dimensionless 3×3 matrix that gives masses to the charged leptons, Z_{ij} is a symmetric complex dimensionless 3×3 matrix that gives Majorana masses to the neutrinos and M is a high energy scale. The selection rule implies

$$\begin{aligned} H(L_i) + H(E_j) + H(H_d) = n &\implies Y_{ij} = O(\lambda^n) \\ H(L_i) + H(L_j) + 2H(H_u) = m &\implies Z_{ij} = O(\lambda^m) \end{aligned} \quad (8.4)$$

where we assume that the horizontal charges of all the superfields are non-negative integers. We learn that the dimensionless couplings that are naively of order unity are suppressed by powers of a small parameter.

Next we demonstrate a realization of the neutrino anarchy scenario using the above framework. Consider the following set of $U(1)_H$ charge assignments

$$\begin{aligned} H(H_u) = 0, \quad H(H_d) = 0, \\ H(L_1) = 0, \quad H(L_2) = 0, \quad H(L_3) = 0, \\ H(E_1) = 8, \quad H(E_2) = 5, \quad H(E_3) = 3. \end{aligned} \quad (8.5)$$

Then, the lepton mass matrices have the following forms

$$M^\ell \sim \langle H_d \rangle \begin{pmatrix} \lambda^8 & \lambda^5 & \lambda^3 \\ \lambda^8 & \lambda^5 & \lambda^3 \\ \lambda^8 & \lambda^5 & \lambda^3 \end{pmatrix}, \quad M^\nu \sim \frac{\langle H_u \rangle^2}{M} \begin{pmatrix} 1 & 1 & 1 \\ 1 & 1 & 1 \\ 1 & 1 & 1 \end{pmatrix}. \quad (8.6)$$

We emphasize that the sign “ \sim ” implies that we only give the order of magnitude of the various entries; there is an unknown (complex) coefficient of $O(1)$ in each entry that we do not write explicitly. Eq. (8.6) predicts large mixing angles

$$\sin \theta_{23} \sim 1, \quad \sin \theta_{12} \sim 1, \quad \sin \theta_{13} \sim 1, \quad (8.7)$$

non-hierarchical neutrino masses

$$m_1^\nu \sim \frac{\langle H_u \rangle^2}{M}, \quad m_2^\nu \sim \frac{\langle H_u \rangle^2}{M}, \quad m_3^\nu \sim \frac{\langle H_u \rangle^2}{M}, \quad (8.8)$$

and hierarchical charged lepton masses

$$m_e \sim \langle H_d \rangle \lambda^8, \quad m_\mu \sim \langle H_d \rangle \lambda^5, \quad m_\tau \sim \langle H_d \rangle \lambda^3. \quad (8.9)$$

We see that this model predicts neutrino masses and mixing angles that are in accordance with the neutrino anarchy scenario. When we assume that both $\langle H_d \rangle$ and $\langle H_u \rangle$ are at the weak scale and that $\lambda \sim 0.2$, this model also reproduces the order of magnitude of the observed charged lepton masses.

Other, more complicated, flavor structure can also be generated using a similar framework. See [2, 4] for more details.

IX. CONCLUSIONS

Neutrino physics is important since it is a tool for probing unknown physics at very short distances. Since we know that the SM has to be extended, it is of great interest to search for such new physics. In general, new physics at high scale predicts massive neutrinos. Therefore, there is a strong theoretical motivation to look for neutrino masses.

In recent years various neutrino oscillation experiments found strong evidences for neutrino masses and mixing

- Atmospheric neutrinos show deviation from the expected ratio between the fluxes of muon neutrinos and electron neutrinos. Moreover, the muon neutrino flux has strong zenith angle dependence. The simplest interpretation of these results is that there are $\nu_\mu - \nu_\tau$ oscillations.

- The electron neutrino flux from the Sun is smaller than the theoretical expectation. Furthermore, the suppression is energy dependent. The total neutrino flux, as measured using neutral current reaction by the SNO experiment, agrees with the theoretical expectation. The simplest interpretation of these results is that there are $\nu_e - \nu_x$ oscillations, where ν_x can be any combination of ν_μ and ν_τ .
- The K2K long baseline experiments found indications for muon neutrino disappearance. Moreover, the same neutrino parameters that account for the atmospheric neutrino disappearance also explain the K2K data.
- The KamLAND experiment found evidences for $\bar{\nu}_e$ disappearance. The data provide an independent test of the same parameter space that is probed by solar neutrinos.

The theoretical expectation and the experimental data fit comfortably. Yet, there are many unsolved problems associated with neutrino physics. In the future we expect to have more data and thus we will be able to learn more about neutrinos, and eventually, about the short distance new physics.

Acknowledgments

I thank Yossi Nir, Subhendu Rakshit, Sourov Roy, Ze'ev Surujon and Jure Zupan for comments on the manuscript. Y.G. is supported by the United States–Israel Binational Science Foundation through Grant No. 2000133, by a Grant from the G.I.F., the German–Israeli Foundation for Scientific Research and Development, and by the Israel Science Foundation under Grant No. 237/01.

[1] A partial list of books includes:

B. Kayser, “The physics of massive neutrinos”, 1989, World Scientific;

J. N. Bahcall, “Neutrino astrophysics”, 1989, Cambridge Univ. Press;

R. N. Mohapatra and P. B. Pal, “Massive neutrinos in physics and astrophysics”, 1991, World Scientific;

C. W. Kim and A. Pevsner, “Neutrinos in physics and astrophysics”, 1993 Harwood Academic;

G. G. Raffelt, “Stars as laboratories for fundamental physics”, 1996, Chicago Univ. Press.

[2] For some recent reviews see:

S. Goswami, hep-ph/0303075;

S. Pakvasa and J. W. Valle, hep-ph/0301061;

- R. N. Mohapatra, hep-ph/0211252;
 E. K. Akhmedov, hep-ph/0001264.
- [3] A. D. Dolgov, hep-ph/0208222; Phys. Rept. **370**, 333 (2002) [hep-ph/0202122].
- [4] M. C. Gonzalez-Garcia and Y. Nir, Rev. Mod. Phys. **75**, 345 (2003) [hep-ph/0202058].
- [5] The neutrino oscillation industry web page: “neutrinooscillation.org”;
 Juha Peltoniemi’s ultimate neutrino page: “cupp oulu.fi/neutrino”.
- [6] Maury Goodman runs the long-baseline neutrino oscillation newsletters. These well written short monthly letters, are very nice summaries of neutrino news. It is highly recommended to sign up for the free monthly email service for anyone who likes to keep up with the developments in neutrino physics. “www.hep.anl.gov/ndk/longbnews/index.html”
- [7] See, e.g., M. E. Peskin and D. V. Schroeder, “Introduction to quantum field theory”, 1995, Addison-Wesley.
- [8] K. Hagiwara *et al.* [Particle Data Group Collaboration], Phys. Rev. D **66**, 010001 (2002).
- [9] H. V. Klapdor-Kleingrothaus *et al.*, Eur. Phys. J. A **12** 147 (2001).
- [10] Y. Grossman and H. J. Lipkin, Phys. Rev. D **55**, 2760 (1997) [hep-ph/9607201].
- [11] L. Wolfenstein, Phys. Rev. D **17**, 2369 (1978).
- [12] See, e.g., H. Nunokawa, V. B. Semikoz, A. Y. Smirnov and J. W. Valle, Nucl. Phys. B **501**, 17 (1997) [hep-ph/9701420];
 S. Bergmann, Y. Grossman and E. Nardi, Phys. Rev. D **60**, 093008 (1999) [hep-ph/9903517].
- [13] S. P. Mikheev and A. Y. Smirnov, Sov. J. Nucl. Phys. **42**, 913 (1985) [Yad. Fiz. **42**, 1441 (1985)].
- [14] S. J. Parke, Phys. Rev. Lett. **57**, 1275 (1986).
- [15] J. Bahcall web site, “www.sns.ias.edu/~jnb”
- [16] See, for example, E. K. Akhmedov, Pramana **54**, 47 (2000) [hep-ph/9907435]; S. T. Petcov, Phys. Lett. B **434**, 321 (1998) [hep-ph/9805262].
- [17] R. Jr. Davis, D. S. Harmer and K. C. Hoffman, Phys. Rev. Lett. **20**, 1205 (1968).
- [18] B. T. Cleveland *et al.*, Astrophys. J. **496**, 505 (1998);
 K. Lande *et al.*, Nucl. Phys. Proc. Suppl. **77**, 13 (1999).
- [19] GALLEX home page: “kosmopc.mpi-hd.mpg.de/gallex/gallex.htm”
- [20] GNO home page: “www.lngs.infn.it/site/exppro/gno/Gno_home.htm”
- [21] SuperKamiokande home page: “www-sk.icrr.u-tokyo.ac.jp/doc/sk/index.html”
- [22] SNO home page: “www.sno.phy.queensu.ca”
- [23] Q. R. Ahmad *et al.* [SNO Collaboration], Phys. Rev. Lett. **89** 011302 (2002) [nucl-ex/0204009].
- [24] See, for example, S. Pakvasa, Pramana **54**, 65 (2000) [hep-ph/9910246].
- [25] P. C. de Holanda and A. Y. Smirnov, hep-ph/0212270;

- J. N. Bahcall, M. C. Gonzalez-Garcia and C. Pena-Garay, hep-ph/0212147;
A. Bandyopadhyay, S. Choubey, R. Gandhi, S. Goswami and D. P. Roy, hep-ph/0212146;
V. Barger and D. Marfatia, Phys. Lett. B **555**, 144 (2003) [hep-ph/0212126].
- [26] A. Bandyopadhyay, S. Choubey, S. Goswami and K. Kar, Phys. Lett. B **519**, 83 (2001) [hep-ph/0106264].
- [27] T. Toshito [Super-Kamiokande Collaboration], hep-ex/0105023.
- [28] S. Fukuda *et al.* [Super-Kamiokande Collaboration], Phys. Rev. Lett. **85**, 3999 (2000) [hep-ex/0009001].
- [29] K2K home page: “neutrino.kek.jp”
- [30] KamLAND home page: “www.awa.tohoku.ac.jp/html/KamLAND/index.html”
- [31] LSND home page: “www.neutrino.lanl.gov/LSND”
- [32] M. H. Ahn *et al.* [K2K Collaboration], Phys. Rev. Lett. **90**, 041801 (2003) [hep-ex/0212007].
- [33] K. Eguchi *et al.* [KamLAND Collaboration], Phys. Rev. Lett. **90**, 021802 (2003) [hep-ex/0212021].
- [34] Karmen home page: “www-ik.fzk.de/~karmen/karmen_e.html”
- [35] MiniBooNE home page: “www-boone.fnal.gov/publicpages/index.html”
- [36] A. de Gouvea and H. Murayama, hep-ph/0301050;
N. Haba and H. Murayama, Phys. Rev. D **63**, 053010 (2001) [hep-ph/0009174];
L. J. Hall, H. Murayama and N. Weiner, Phys. Rev. Lett. **84**, 2572 (2000) [hep-ph/9911341].
- [37] For a review see, for example, R. N. Mohapatra, hep-ph/9910365.
- [38] For a recent paper see, for example, C. Giunti, hep-ph/0302173.
- [39] M. Leurer, Y. Nir and N. Seiberg, Nucl. Phys. B **398**, 319 (1993) [hep-ph/9212278];
M. Leurer, Y. Nir and N. Seiberg, Nucl. Phys. B **420**, 468 (1994) [hep-ph/9310320];
Y. Grossman and Y. Nir, Nucl. Phys. B **448**, 30 (1995) [hep-ph/9502418].